25th ABCM International Congress of Mechanical Engineering
October 20-25, 2019, Uberlândia, MG, Brazil

COB-2019-0404
DIMENSIONAL SYNTHESIS OF COMPLEX GEAR TRAINS FOR RAPID PROTOTYPING WITH 3D PRINTING

Marina Baldissera de Souza
Virgílio Silveira Lima
Rodrigo de Souza Vieira
Daniel Martins
Universidade Federal de Santa Catarina, Departamento de Engenharia Mecânica, Centro Tecnológico, Campus Universitário - Trindade, CEP: 88.040-900, Florianópolis/SC - Brasil
marina.bs@posgrad.ufsc.br - v.s.lima@grad.ufsc.br - rodrigo.vieira@ufsc.br - daniel.martins@ufsc.br

Abstract. *Planetary gear trains (PGT) are largely used in industry due to their features such as high torque capacity, lower weight and highly compact package. The wide range of application of PGTs has led to the development of synthesis methodologies. Most of these methodologies focus on the generation of different topologies, usually ending with a schematic representation. In these works, other stages of the design conception are not carried out, e.g. the dimensional synthesis. The optimization researches to size PGTs found in literature, in spite of being very complete, have as starting point a simple and not innovative architecture. This paper aims to run against this trend, proposing a technique for dimensional synthesis of a complex PGT. The dimensional synthesis is done via Davies' method, based on graph and screw theories. Through the Davies method, an optimization problem is built, where the objective function is related to the PGT's ratio and the design variables are the number of teeth and the modules of the gears. Using the Differential Evolution algorithm to solve the optimization problem, the number of teeth and modules that give a target ratio are obtained. Then, the PGT is modeled in a CAD software and a prototype will be 3D printed to physically represent it.*

Keywords: *planetary gear train, dimensional synthesis, optimization, Davies' method, rapid prototyping*

1. INTRODUCTION

Planetary gear trains (PGT) are found in automobile transmissions, differential gears, machine tool gearboxes, robot manipulators and so on. This class of mechanism has been largely used in industry due to their features, among which high torque capacity, lower weight and highly compact package are included.

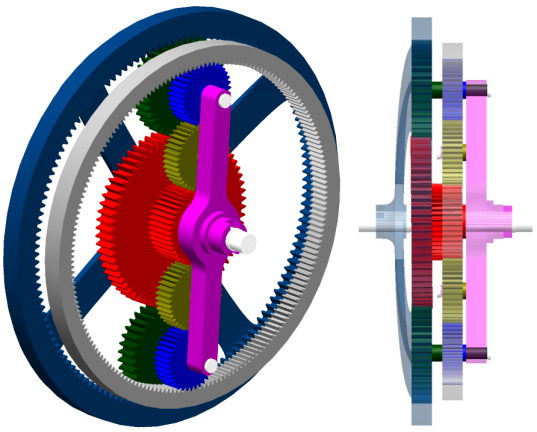

Figure 1: Isometric view and side view of the PGT to be sized and printed.

Methodologies for the synthesis of PGTs have been developed since the 1970's, supported by graph theory (Buchsbaum and Freudenstein, 1970). Most of these works focus on the number synthesis or enumeration of graphs to generate the maximum possible amount of PGTs with different topologies, aiming to obtain a structure with potential for patenting. However, the development of the PGT usually ends with a schematic representation and the conception is interrupted. Other stages of the methodology for the development of mechanisms with an innovative design are not carried out, such as

dimensional synthesis and prototyping (Murai *et al.*, 2013). Even very complete works do not present a sizing technique for the synthesized PGT. For example, Salgado and Del Castillo (2014) enumerated the kinematic inversions of the PGTs with four, five and six links and determined their transmission ratio and efficiency ranges. The design process finishes with the generation of schematic representations of the best topologies, without providing the number of teeth and module of the PGTs.

The dimensional synthesis techniques found in the literature are done via optimization. Most of optimization works focus on multi-stage gear trains, such as the ones listed by Golabi *et al.* (2014). The few optimization problems built for PGTs normally aim to minimize the volume and optimize other characteristics, as load sharing performance or efficiency. Other aspects, such as contact and bending stresses and tooth thickness, are covered by the constraint functions. The number of teeth and module are among the design variables, therefore the minimizer of the objective function defines the PGT's dimensions (Stefanović-Marinović *et al.*, 2017; Salgado *et al.*, 2017; Zhang *et al.*, 2018). In spite of being very complete, these techniques are made for PGTs with simple and not innovative architectures.

This paper aims to run against these trends, presenting a technique for the dimensional synthesis of a PGT with complex architecture which will be rapid prototyped in a 3D printer. The PGT to be sized and printed is an adaptation of the gear train synthesized in Souza *et al.* (2018) and is shown in Fig. 1. The technique is based on the Davies method, a method associating graph and screw theories. The sizing technique has the advantage of being generic: it can be applied to any PGT's architecture without restriction. Other advantage of this technique is generating an analytical expression of the final ratio of a PGT from a short and systematic description of its geometry. By associating the Davies method with an optimization algorithm, this technique of dimensional synthesis gives the number of teeth and the module the gears composing the PGT should have to obtain a desired final ratio. After the dimensional synthesis, the PGT is modeled in a CAD software to print a prototype. A motion simulation is also carried out to verify if the PGT sized with the optimization solution presents the desired ratio.

The remainder of this paper is structured as follows. Section 2. briefly reviews how the Davies method associates graph and screw theories to perform the kinematic analysis of mechanisms. The PGT to have its dimensions defined is described in detail in Section 3.. The dimensional synthesis process, the optimization problem construction and its solution are explained and analyzed in Section 4. Section 5.presents the steps of the development of the CAD model and the verification if the values obtained in the optimization give the desired ratio. Finally, some considerations about the results achieved in this paper are made in Section 6.

2. KINEMATIC ANALYSIS USING GRAPH AND SCREW THEORIES

To carry out the kinematic analysis of mechanisms, Davies (1981) presented an equivalent for the Kirchhoff Voltage Law for a network of links (bodies) and couplings, based on graph and screw theories. In this adaptation, a multibody system is represented by a graph, whose edge variables model the motions allowed by the couplings. This analogy is called Davies' method (Cazangi, 2008).

2.1 Concepts of graph theory used in the Davies method

Any mechanism can be represented by a graph, whose nodes stand for the links and whose edges stand for the couplings. The resulting graph is called *coupling graph*. When the edges are oriented from one node to another, the graph is called a directed graph or a di-graph.

A *spanning tree* is a subgraph containing a subset of edges connecting all the nodes of the graph. The edges of the spanning tree are called branches and the remaining edges of the graph are called chords. A *fundamental circuit* is closed when a chord is added to the spanning tree. There is a single fundamental circuit for each chord, i.e., the number ν of fundamental circuits is equal to the number of chords. The number of fundamental circuits is defined by $\nu = e - n + 1$, where n is the number of links/nodes and e is the number of couplings/edges.

The chords generating the fundamental circuit defines the orientation of the circuit. The fundamental circuits of a di-graph are mathematically represented by the *fundamental circuit matrix* $[B]_{\nu \times e}$, whose elements $b_{i,j}$ are defined by the following rule:

- $b_{i,j} = 1$ if e_j belongs to the fundamental circuit ν_i and it follows the orientation defined by the closing chord;
- $b_{i,j} = -1$ if e_j belongs to the fundamental circuit ν_i and its orientation is opposed to the one defined by the closing chord;
- $b_{i,j} = 0$ if e_j does not belong to the fundamental circuit ν_i.

The expansion of the graph's edges according to the degrees of freedom of the couplings they represent generates the *motion graph*. The fundamental circuit matrix can also be constructed from the motion graph, resulting in a matrix $[B_M]_{\nu \times F}$. F is the *gross degree of freedom* of the mechanism represented by the motion graph and it is the sum of all the independent unitary motions allowed by each coupling f_i:

$$F = \sum_{i=1}^{e} f_i \tag{1}$$

The association of these concepts with screw theory to carry out the kinematic analysis of a mechanism is presented in Section 2.2.

2.2 Screw theory applied to kinematic analysis of mechanisms

A *screw* $\$$ is a geometrical element which can represent mechanical quantities. It is defined by a straight line (instantaneous screw axis - ISA) and an associated pitch h, with unit of length. A *normalized screw* $\hat{\$}$ has a unitary vector standing for the ISA. For kinematics, a screw system is composed of all screw axes of motions allowed by the couplings of the mechanism. All possible motions are described by this system (Waldron and Hunt, 1991). The screw system corresponds to the space where the coupling is represented. For kinematics, the *order of the screw system* λ is the smallest dimension able to represent the set of motions of the couplings. For example, in a planar space, $\lambda = 3$, since the set of motions are described with two translations and one rotation.

In kinematic analysis, the instantaneous state of motion of a rigid body, in respect to an inertial system with coordinates O_{xyz}, is described by a screw called *twist* $\$^m$. The twist is a combination of an angular velocity ω around the ISA and a linear velocity τ on the same axis. The twist's pitch is defined by the ratio $h = \tau/\omega$. The twist is composed by an angular velocity vector $\vec{\omega} = \{r, s, t\}$ and a linear velocity vector $\vec{V_P} = \{u, v, w\}$. The twist is organized in axis formation:

$$\$^m = \begin{pmatrix} \vec{\omega} \\ \hline \vec{V}_P \end{pmatrix} = \begin{pmatrix} r \\ s \\ t \\ \hline u \\ v \\ w \end{pmatrix} = \begin{pmatrix} \vec{\omega} \\ \hline \vec{S_0} \times \vec{\omega} + h\vec{\omega} \end{pmatrix} = |\vec{\omega}| \begin{pmatrix} \vec{S}^M \\ \hline \vec{S_0} \times \vec{S}^M + h\vec{S}^M \end{pmatrix} \tag{2}$$

The unit vector $\vec{S}^M$ defines the direction of the twist's ISA and $\vec{S_0}$ is the position vector of any point on the twist's axis regarding O_{xyz}. $\vec{V}_P$ comes from the sum of the parallel velocity to the ISA ($h\vec{\omega}$) and the normal velocity to the ISA ($\vec{S_0} \times \vec{\omega}$). A pure angular velocity has $h = 0$ and a pure linear velocity has $h \to \infty$.

The angular velocity magnitude $|\vec{\omega}| = \sqrt{r^2 + s^2 + t^2}$ gives the magnitude φ^m of the twist when h does not tend to infinity. Otherwise, φ^m is given by the linear velocity magnitude $\left|\vec{V_P}\right| = \sqrt{u^2 + v^2 + w^2}$ when $h \to \infty$. φ^m is used to normalize the twist: $\$^m = \varphi^m \hat{\$}^m$.

By disposing side by the twists, the *motion matrix* is generated: $[M_D]_{\lambda \times F} = \left[\begin{array}{cccc} \$_a^m & \$_b^m & \cdots & \$_F^m \end{array} \right]$. If the twists are normalized, the *unit motion matrix* $[\hat{M}_D]_{\lambda \times F}$ is created: $[\hat{M}_D]_{\lambda \times F} = \left[\begin{array}{cccc} \hat{\$}_a^m & \hat{\$}_b^m & \cdots & \hat{\$}_F^m \end{array} \right]$. The magnitude of the twists are contained in the vector $\{\vec{\psi}\}_{F \times 1} = \left\{ \begin{array}{cccc} \varphi_a^m & \varphi_b^m & \cdots & \varphi_F^m \end{array} \right\}^T$.

Relations among the motions allowed by the couplings belonging to the same circuit are established using an analogy with the Kirchhoff's Voltage Law. The Kirchhoff's Voltage Law states that the algebraic sum of the electrical potential differences around any closed network is zero. Analogously, the algebraic sum of the twists around any circuit is zero. Each one of the λ components of the twists belonging to a circuit must have its sum equals to zero. This is mathematically translated by doing ν times the product between $[\hat{M}_D]_{\lambda \times F}$ and a diagonal matrix composed of the elements of each row of $[B_M]_{\nu \times F}$. That operation gives the *network unit motion matrix* $[\hat{M}_N]_{\lambda\nu \times F}$. This matrix is the coefficient matrix of an homogeneous linear system, whose set of unknowns are the elements of $\{\vec{\psi}\}_{F \times 1}$. This statement can be mathematically written as:

$$[\hat{M}_N]_{\lambda.\nu \times F} \{\vec{\psi}\}_{F \times 1} = \{\vec{0}\}_{\lambda.\nu \times 1} \tag{3}$$

The F unknown variables related by the $\lambda.\nu$ equations are written as function of a subset of F_N known variables, called *primary variables*. F_N is the *net degree of freedom* and it is determined by the difference between F and the rank m of the matrix $[\hat{M}_N]_{\lambda.\nu \times F}$. The remaining m unknown variables are designated as *secondary variables*. The value of F_N establishes the number of variables that must be imposed in order to solve the homogeneous linear system of Eq, (3), giving the solution of the kinematic analysis.

3. STRUCTURE OF THE PLANETARY GEAR TRAIN

This paper is a continuation of the synthesis started in (Souza *et al.*, 2017) and (Souza *et al.*, 2018), where graphs are enumerated to generate a PGT from a kinematic chain belonging to a minimal set. Figure 2 shows the CAD model of

an adaptation of the PGT generated in (Souza *et al.*, 2018). The schematic representation of the PGT shown in Fig. 2 is depicted in Fig. 3. Figure 4 contains the di-graph representing the PGT, where the dashed edges stand for gear pairs and the full edges stand for revolute pairs. For the application of the Davies method, the bodies of the PGT are numbered from 0 to 6 and its joints are labelled from A to K, as shown in Fig. 2 and 3. The pitch radium r_i of gear i is also represented in Fig. 3. The identification of the bodies (links) composing the PGT are shown in Tab. 1 and the joints are described in Tab. 2.

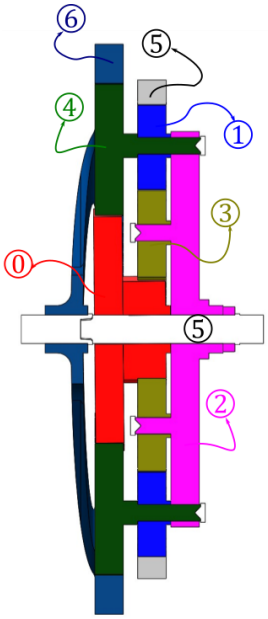

Figure 2: CAD model of the adaptation of the PGT created in (Souza *et al.*, 2018).

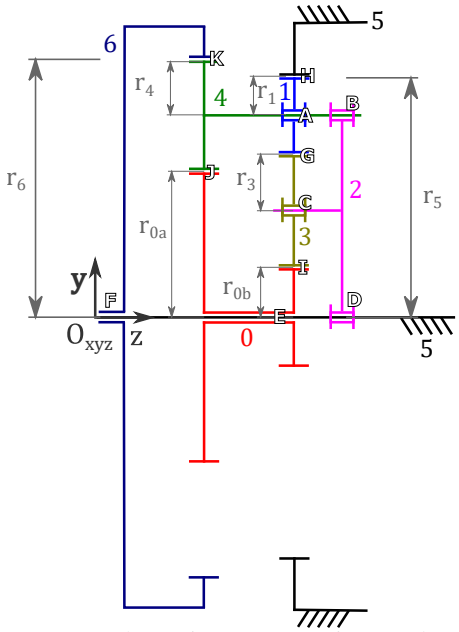

Figure 3: PGT's schematic representation. Adapted from: Souza *et al.* (2018).

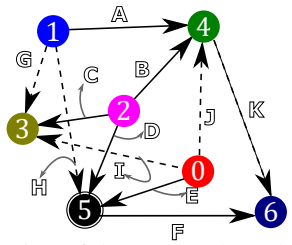

Figure 4: Graph representation of the PGT. Adapted from: Souza *et al.* (2018).

Table 1: Identification of the PGT's links

Link number	PGT's rigid body
0	Sun gear
1	Planet gear (second stage)
2	Carrier
3	Planet gear (first stage)
4	Planet gear
5	Ring gear (fixed link)
6	Ring gear

Considering the coordinate system O_{xyz} in Fig. 3, it is assumed that the PGT occupies negligible axial length, that the gears are thin spur gears whose tooth contacts lie on the y axis and that the pressure angle is zero. The only motion allowed by the kinematic pairs is an angular velocity with magnitude t around the z axis on the plane $x = 0$, so all the twists have their direction defined by $\vec{S}^M = [0, 0, 1]^T$ and $h = 0$. Thus the twists belong to the 2^{nd} special 2-system of screws (Hunt, 1978) i.e. the order of the screw system is $\lambda = 2$ (Laus *et al.*, 2012). Due to these simplifying hypotheses, only the y coordinates of the couplings are relevant for the Davies method. The other elements of the position vector

Table 2: Identification of the PGT's kinematic pairs

Joint	Pair of links	Kinematic pair	$\vec{S}_0$	Function
A	1,4	Revolute pair	$[0, r_{0_b} + 2r_3 + r_1, 0]^T$	
B	2,4	Revolute pair	$[0, r_{0_a} + r_4, 0]^T$	
C	2,3	Revolute pair	$[0, r_{0_b} + r_3, 0]^T$	
D	2,5	Revolute pair	$[0, 0, 0]^T$	Input
E	0,5	Revolute pair	$[0, 0, 0]^T$	
F	5,6	Revolute pair	$[0, 0, 0]^T$	Output
G	1,3	Gear pair	$[0, r_{0_b} + 2r_3, 0]^T$	
H	1,5	Gear pair	$[0, r_{0_b} + 2r_3 + 2r_1, 0]^T$	
I	0,3	Gear pair	$[0, r_{0_b}, 0]^T$	
J	0,4	Gear pair	$[0, r_{0_a}, 0]^T$	
K	4,6	Gear pair	$[0, r_{0_a} + 2r_4, 0]^T$	

can be null, as shown in the fourth column of Tab. 2, which contains the position vectors of the couplings. Thus, all the information needed to build the twists according to Eq. (2) are available.

The PGT has $n = 7$ links and $e = 11$ joints, thus the di-graph of Fig. 4 has $\nu = 11 - 7 + 1 = 5$ fundamental circuits. Since all the kinematic pairs of the PGT have one degree-of-freedom ($f_i = 1$), the gross degree of freedom of the PGT is $F = 11$ and the PGT's motion graph is identical to the di-graph of Fig. 4. Taking the dashed edges as chords, the di-graph is used to create the fundamental circuit matrix $[B_M]_{5\times11}$, using the rule of Section 2.1:

$$[B_M]_{5\times11} = \begin{array}{c} \begin{matrix} A & B & C & D & E & F & G & H & I & J & K \end{matrix} \\ \begin{bmatrix} -1 & 1 & -1 & 0 & 0 & 0 & 1 & 0 & 0 & 0 & 0 \\ -1 & 1 & 0 & -1 & 0 & 0 & 0 & 1 & 0 & 0 & 0 \\ 0 & 0 & -1 & 1 & -1 & 0 & 0 & 0 & 1 & 0 & 0 \\ 0 & -1 & 0 & 1 & -1 & 0 & 0 & 0 & 0 & 1 & 0 \\ 0 & 1 & 0 & -1 & 0 & -1 & 0 & 0 & 0 & 0 & 1 \end{bmatrix} \end{array} \begin{matrix} \\ \nu_G \\ \nu_H \\ \nu_I \\ \nu_J \\ \nu_K \end{matrix} \tag{4}$$

After building the twists and $[B_M]_{5\times11}$, the homogeneous linear system of Eq. (3) is constructed. The variables of the linear system are the magnitudes t of the couplings' angular velocities. The rank of the resulting matrix $[\hat{M}_N]_{10\times11}$ is $m = 10$, so the PGT has $F_N = F - m = 11 - 10 = 1$ degree of freedom. The magnitude t_D of the angular velocity of coupling D, the PGT's input, is the primary variable to solve the linear system. Therefore, the carrier 2 is the input link of the PGT. A value of $t_D = 1$ rad/s is adopted as input speed.

4. DIMENSIONAL SYNTHESIS

From Tab. 2, it can be noted that the couplings' position depends on the pitch radii of the gears. Thus the solution of the kinematic analysis gives the angular velocities' magnitudes as function of the pitch radii, leading to an analytic expression f_{ratio} of the PGT's ratio. Values of the gears' pitch radii giving a desired PGT's ratio can be found by using this analytic expression as the core of an objective function of an optimization problem.

4.1 Objective function

The moving ring gear (link 6) is the PGT's output link, thus the angular velocity t_F is the PGT's output speed. The solution of Eq. (3) defines t_F as function of the pitch radii of the gears, i.e. $t_F = f(r_i), i = 0...6$. Dividing the output speed t_F by the input speed t_D gives the PGT's final ratio $f_{ratio} = f(r_i), i = 0...6$. However, f_{ratio} can be rewritten as function of the module of the gears and the number of teeth. Considering that gear 4 and the left side of gear 0 have a module of m_1, their pitch radii is defined as $r_i = m_1 z_i/2$, for $i = 0_a, 4$. Similarly, considering that gears 1 and 3 and the right side of gear 0 have module of m_2, the product $r_i = m_2 z_i/2$, for $i = 0_b, 1, 3$, defines their pitch radii.

Having the carrier as the input link (link 2) and the moving ring gear (link 6) as the output link, the PGT's ratio is determined as $f_{ratio} = f(m_1, m_2, z_i), i = 0...6$:

$$f_{ratio} = \frac{t_F}{t_D} = \frac{-2(-m_2 z_1^2 z_{0_a} - 3m_2 z_1 z_3 z_{0_a} + m_1 z_1 z_{0_a}^2 - m_2 z_1 z_{0_a} z_{0_b} + 2m_1 z_4 z_1 z_{0_a} + m_2 z_4 z_1 z_{0_b})}{z_{0_b}(2z_4 + z_{0_a})(m_2 z_1 + 2m_2 z_3 - m_1 z_{0_a} + m_2 z_{0_b})} + \\ + \frac{-2(-2m_2 z_3^2 z_{0_a} + m_1 z_3 z_{0_a}^2 - m_2 z_3 z_{0_a} z_{0_b} + 2m_1 z_4 z_3 z_{0_a} + 2m_2 z_4 z_3 z_{0_b} + m_2 z_4 z_{0_b}^2)}{z_{0_b}(2z_4 + z_{0_a})(m_2 z_1 + 2m_2 z_3 - m_1 z_{0_a} + m_2 z_{0_b})} \quad (5)$$

The objective function of an optimization problem where the design variables are the number of teeth and the modules is built from f_{ratio}. The objective function is defined as the absolute value of the difference between the numerical value of the desired ratio and f_{ratio}. Supposing a desired ratio of $I_{target} = -3$, the objective function of the optimization problem can be written as (Souza, 2018):

$$f_{obj} = |I_{target} - f_{ratio}| = |-3 - f_{ratio}| = f(\vec{x}) = f(m_1, m_2, z_{0_a}, z_{0_b}, z_1, z_3, z_4) \quad (6)$$

where $\vec{x} = \{m_1, m_2, z_{0_a}, z_{0_b}, z_1, z_3, z_4\}^T$ is a vector containing the design variables of the optimization problem.

4.2 Constraint functions

The objective function is subject to the following constraint functions:

i The minimum number of teeth for gears 0_a, 0_b, 1, 3 and 4 is 17 (Zhang *et al.*, 2018);

ii The maximum number of teeth for gears 0_a, 0_b, 1, 3 and 4 is 136;

iii The number of teeth must be an integer number, i.e. $z_i \in \mathbb{Z}, i = 0...6$;

iv The minimum value of m_1 and m_2 is 1 mm, minimum suitable value to print a PGT with a good motion transmission;

v The modules m_1 and m_2 must assume standard values inside the range: [1, 1.25, 1.5, 2, 3, 4, 5] (Norton, 2010);

vi The gears' pitch diameter must be greater than 30 mm;

vii The pitch diameter of the ring gears (links 5 and 6) must not exceed 230 mm, to fit on the print bed of the 3D printer;

viii The axes of gear 4 and gear 1 must be aligned, i.e.:

$$r_{0_a} + r_4 = r_{0_b} + 2r_3 + r_1 \quad (7)$$

A tolerance of $\epsilon = 10^{-4}$ is adopted for constraints iii, v and viii. The constraint functions are incorporated to the optimization problem via penalization of the objective function. The weight factor in the objective function penalization is defined as 10 by trial and error.

4.3 Results and analysis

The genetic algorithm of the Differential Evolution (DE) is used to solve the optimization problem (Das and Suganthan, 2011). The DE algorithm gives the gears' number of teeth and modules that makes the difference of Eq. (6) as close as possible to zero. The algorithm stops if $|I_{target} - f_{ratio}| \leq 10^{-2}$ or the number of iterations exceeds 10000. After reaching the maximum value of iterations, the algorithm stops at the local minimizer presented in Tab. 3.

Table 3: Local minimizer of the objective function

z_{0_a}	z_{0_b}	z_1	z_3	z_4	m_1 [mm]	m_2 [mm]
65.9999	43.0001	35.0001	38.0001	36.9999	1.4999	1.0032

In order to model the PGT on a CAD software, the values of Tab. 3 regarding the number of teeth are rounded to the closest integer. Moreover, the modules m_1 and m_2 are rounded to the closest standard metric value. The rounded values are shown in Tab. 4.

Substituting the values of Tab. 3 in Eq. (5) gives a ratio of -3.0721. The resulting ratio diverges from the target value by around 2.4%. The rounded values of Tab. 4 increase the discrepancy between the resulting ratio and the target value. Applying them in Eq. (5) gives $f_{ratio} = -3.1098$, diverging by around 3.4% of I_{target}.

Constraint viii is also verified: using the minimizer shown in Tab. 3 in Eq. (7) results in a difference of 10^{-4} mm between the left side and the right side of the equation, thus respecting the adopted tolerance. In contrast, the difference

Table 4: Number of teeth and modules of the gears composing the PGT

z_{0_a}	z_{0_b}	z_1	z_3	z_4	m_1 [mm]	m_2 [mm]
66	43	35	38	37	1.5	1

between the left and right sides of Eq. (7) increases to 0.25 mm when the rounded values of Tab. 4 are applied, surpassing the admitted tolerance of $\epsilon = 10^{-4}$.

The main source of the errors described herein is the definition of the constraint functions. The fact that the maximum number of iterations were reached before all stop criteria being satisfied highlights that meeting all the constraints guaranteeing that the PGT's ratio achieves I_{target} is difficult. Restraining the design variables to integer (number of teeth) or discrete (module) values is a complicating factor. The rounding to obtain the values of Tab. 4 amplifies the errors coming from not meeting all the constraints.

Some modifications in the constraint functions could be done to obtain a more precise solution. The rounding error could be decreased by reducing the tolerance ϵ. This would result in m_1 and m_2 closer to standard metric values and $z_i, i = 0...6$ closer to integer numbers. Another modification is adopting different tolerances for constraints iii, v and viii, instead of using a single value for all of them. The constraint presenting the highest impact on the optimization solution should have the smallest tolerance.

Despite of ratio and center-distance errors coming from the optimization and the rounding of the local minimizer, the values of Tab. 4 are used to build the CAD model. One of the main advantages of the involute tooth form is that center-distance errors do not affect the velocity ratio (Norton, 2010). Moreover, the machine that will print the PGT can generate printing errors greater than 0.25 mm. For these reasons, since the objective of this paper is just to create a physical model of the PGT whose sizing considered only the velocity ratio, these errors can be neglected.

5. CAD MODEL FOR 3D PRINTING

The CAD model was made in SOLIDWORKS 2019 (SW), using the SOLIDWORKS Toolbox. The Toolbox is a digital library with several predefined norms and standardization, being possible to define the part properties and their dimensions in a simple way through the Property Manager function (SOLIDWORKS, 2018).

In this paper, using SOLIDWORKS Toolbox, we have created spur gears, external and internal toothed gears, according to the International Standardization Organization (ISO). The input data required for construction are module, number of teeth, pressure angle, face width, hub style, nominal shaft diameter and keyway as shown in Fig. 5.

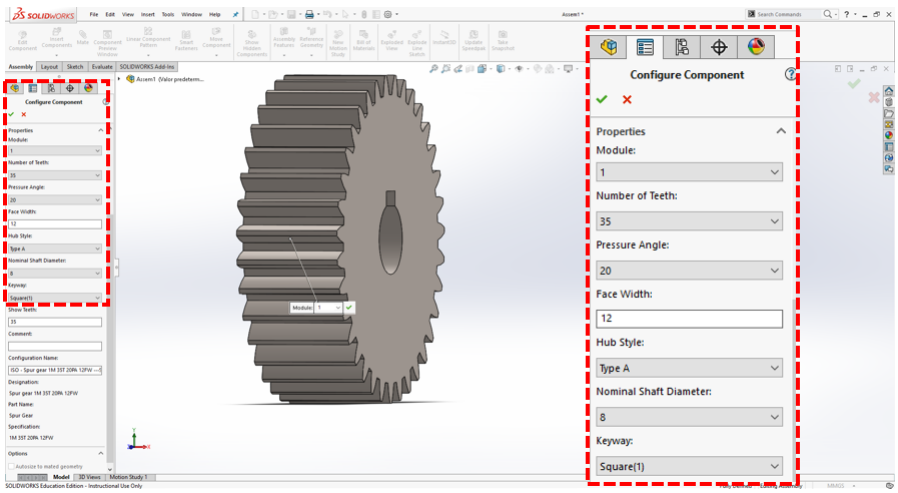

Figure 5: Creation of a gear using the SOLIDWORKS Toolbox with the input data highlighted.

5.1 Modeling

With the main objective for 3D printing on ABS plastic, with stress strengths and resistance much lower than metals, the model has module and number of teeth resulting from the Davies method while other data have been adapted to make the model more aesthetically acceptable. The sizing of the axles is not in the scope of this work, but it will be included in future works. For saving material, the carrier of the PGT was modeled with two arms.

5.2 Positioning

After finishing the model, the mating rules for the motion study were made, such as coincidences of planes, concentric surfaces, locks, and SW mechanical gear positioning, exemplified in Fig. 6.

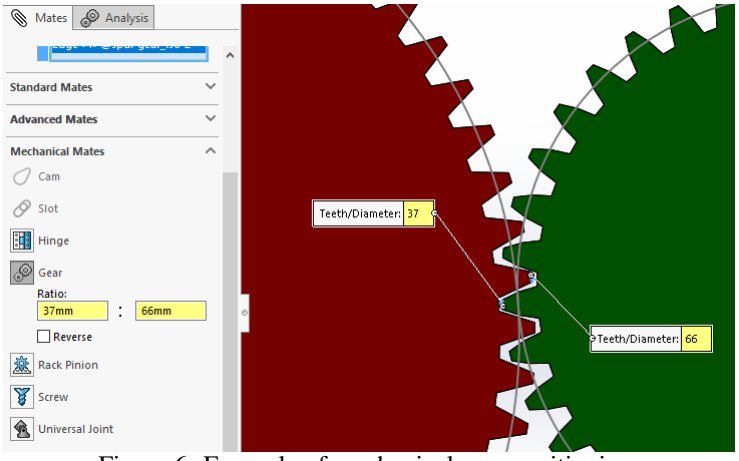

Figure 6: Example of mechanical gear positioning.

5.3 Motion analysis

One of the reasons to use SW is the work validation, because the software simulates and analyzes the motion of an assembly while incorporating the effects of motion study elements. In this case, a motor with constant speed of 20 rpm was simulated, as illustrated in Fig. 7.

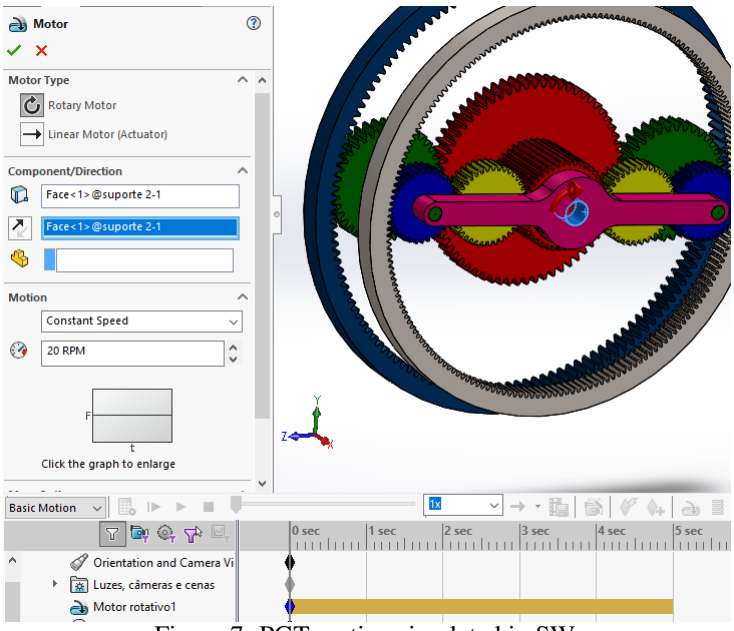

Figure 7: PGT motion simulated in SW.

As a result, a curve of the output speed of the ring gear 6 is generated, shown in Fig. 8. Note that with an input of 20 rpm on carrier 2, the internal spur gear 6 achieves an angular speed of around 368.6 °/s or around 61.4 rpm, as emphasized in Fig. 8. The ratio between the output speed and input speed is around 3.072, very close to the value found in Section 4. 3, as expected. The little divergence between the ratio given by SW and the value defined using Eq. (5) is possibly due to intrinsic truncation and rounding errors of the softwares.

5.4 3D printing modeling

Due to the simplicity of the initial modeling, changes were necessary to enable the construction of a functional prototype in a 3D printer. Acrylic clamping plates were also modeled on SW to help in modeling changes. The result was a

more detailed model, shown in Fig. 9. The model final weight, composed of ABS plastic material and acrylic plates, is about 1.45 kg.

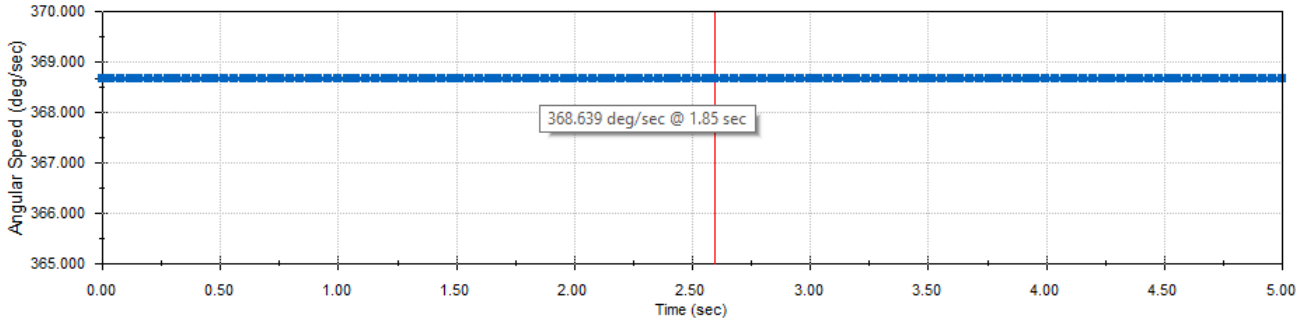

Figure 8: Angular speed of ring gear 6 given by the SW motion analysis.

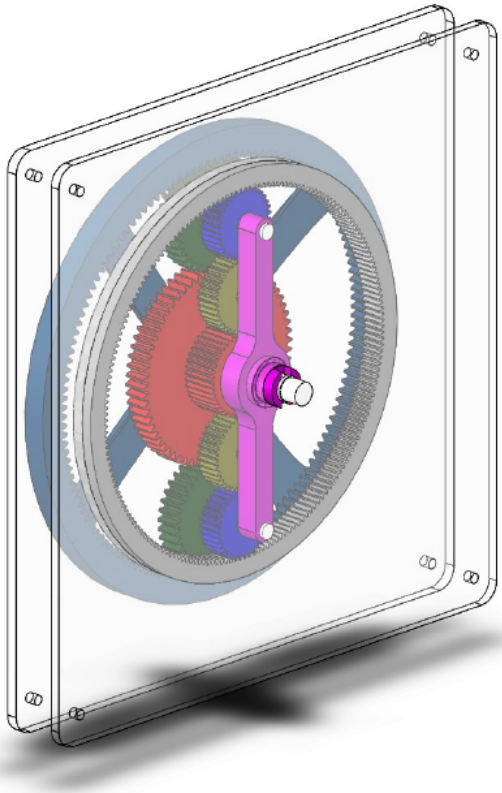

Figure 9: CAD model of the PGT prototype.

6. CONCLUSIONS

This paper presented a technique of dimensional synthesis of a PGT with complex architecture. The technique uses an electromechanical analogy to create the objective function of an optimization problem in order to define the number of teeth and the modules the gears should have so that the PGT achieves a target velocity ratio. After obtaining a solution for the optimization problem, the found values are used as input to model the PGT in a CAD software. The velocity ratio obtained with the optimization solution is verified and a more detailed model is prepared to be 3D printed.

The sizing technique presented some error. However, it must be highlighted that these errors are due to rounding values and the difficulty to converge to a minimizer that respects all the constraint functions. The errors do not come from the Davies method. The Davies method is a powerful tool to size gear trains with complex topology and other mechanisms as it provides a methodical way to construct optimization problems. The Davies method is the reason behind the main advantages of this dimensional synthesis technique: (i) it is a generic technique that can be applied in PGTs

of any architecture without restriction; (ii) it allows to easily generate analytical expressions from a brief and systematic description of the PGT.

Therefore, this dimensional synthesis technique based on Davies method is worth improving. Future works include correcting the mathematical errors by trying the modifications proposed in Section 4.3; making an action analysis in parallel with the kinematic analysis to consider other aspects in the sizing, such as contact and bending stresses; adding some constraint functions to size the axles; carrying out a similar dimensional synthesis process, but based on efficiency; creating a prototype using machine tools after correcting the mathematical errors and expanding the dimensional synthesis technique.

7. ACKNOWLEDGEMENTS

Thanks are due to the National Council for Scientific and Technological Development (CNPq) for financial support. The authors would like to thank the colleague João Vitor Fernandes de Brito, Eng. (UFSC), for providing helpful 3D printer's data, and professor Fabio de Freitas Lima, Dr. Eng. (UTFPR), who provided insight and expertise that greatly assisted this work. Thanks are also due to professor Estevan Hideki Murai (UFSC) and the colleague Davi Henrique Cavilion Lapolli (UTFPR) for helping in the CAD model.

8. REFERENCES

Buchsbaum, F. and Freudenstein, F., 1970. "Synthesis of kinematic structure of geared kinematic chains and other mechanisms". *Journal of mechanisms*, Vol. 5, No. 3, pp. 357–392.

Cazangi, H.R., 2008. *Aplicação do método de Davies para análise cinemática e estática de mecanismos com múltiplos graus de liberdade*. Master's thesis, Universidade Federal de Santa Catarina.

Das, S. and Suganthan, P.N., 2011. "Differential evolution: A survey of the state-of-the-art". *IEEE transactions on evolutionary computation*, Vol. 15, No. 1, pp. 4–31.

Davies, T., 1981. "Kirchhoff's circulation law applied to multi-loop kinematic chains". *Mechanism and machine theory*, Vol. 16, No. 3, pp. 171–183.

Golabi, S., Fesharaki, J.J. and Yazdipoor, M., 2014. "Gear train optimization based on minimum volume/weight design". *Mechanism and machine theory*, Vol. 73, pp. 197–217.

Hunt, K.H., 1978. *Kinematic geometry of mechanisms*, Vol. 7. Oxford University Press, USA.

Laus, L., Simas, H. and Martins, D., 2012. "Efficiency of gear trains determined using graph and screw theories". *Mechanism and Machine Theory*, Vol. 52, pp. 296–325.

Murai, E.H., Martins, D. and Simas, H., 2013. "Number and type syntheses for an one-side stitching device". In *Proceedings of the 22nd International Congress of Mechanical Engineering-COBEM*.

Norton, R.L., 2010. *Machine Design: An Integrated Approach*. Prentice Hall, 4th edition.

Salgado, D. and Del Castillo, J., 2014. "Analysis of the transmission ratio and efficiency ranges of the four-, five-, and six-link planetary gear trains". *Mechanism and Machine Theory*, Vol. 73, pp. 218–243.

Salgado, D., González, A., Sanz-Calcedo, J.G., Beamud, E., García, E. and Núñez, P., 2017. "Optimal design of planetary gearboxes for application in machine tools". *Procedia Manufacturing*, Vol. 13, pp. 267–274.

SOLIDWORKS, 2018. "Biblioteca do toolbox". URL `http://help.solidworks.com/2018/Portuguese-brazilian/SolidWorks/toolbox/c_toobox_browser.htm`. Accessed: 1 jul. 2019.

Souza, M.B., 2018. *Efficiency optimization of a hybrid automotive transmission's gear train using graph and screw theories*. Master's thesis, Universidade Federal de Santa Catarina.

Souza, M.B., Vieira, R.S. and Martins, D., 2017. "Enumeration of kinematic chains with zero variety for epicyclic gear trains with one and two degrees of freedom". In *International Symposium on Multibody Systems and Mechatronics*. Springer, pp. 15–24.

Souza, M.B., Vieira, R.S. and Martins, D., 2018. "Synthesis of epicyclic gear trains with one and two degrees of freedom from kinematic chains belonging to minimal sets". *International Journal of Mechanisms and Robotic Systems*, Vol. 4, No. 4, pp. 383–400.

Stefanović-Marinović, J., Troha, S. and Milovančević, M., 2017. "An application of multicriteria optimization to the two-carrier two-speed planetary gear trains". *Facta Universitatis, Series: Mechanical Engineering*, Vol. 15, No. 1, pp. 85–95.

Waldron, K.J. and Hunt, K.H., 1991. "Series-parallel dualities in actively coordinated mechanisms". *The International Journal of Robotics Research*, Vol. 10, No. 5, pp. 473–480.

Zhang, J., Qin, X., Xie, C., Chen, H. and Jin, L., 2018. "Optimization design on dynamic load sharing performance for an in-wheel motor speed reducer based on genetic algorithm". *Mechanism and Machine Theory*, Vol. 122, pp. 132–147.

9. RESPONSIBILITY NOTICE

The authors are the only responsible for the printed material included in this paper.